MICROBIOLOGY

Accumulation of defense systems in phage-resistant strains of *Pseudomonas aeruginosa*

Ana Rita Costa[1,2]†, Daan F. van den Berg[1,2]†, Jelger Q. Esser[1,2]†, Aswin Muralidharan[1,2], Halewijn van den Bossche[1,2], Boris Estrada Bonilla[1,2], Baltus A. van der Steen[1,2], Anna C. Haagsma[1,2], Ad C. Fluit[3], Franklin L. Nobrega[4], Pieter-Jan Haas[3], Stan J. J. Brouns[1,2]*

Prokaryotes encode multiple distinct anti-phage defense systems in their genomes. However, the impact of carrying a multitude of defense systems on phage resistance remains unclear, especially in a clinical context. Using a collection of antibiotic-resistant clinical strains of *Pseudomonas aeruginosa* and a broad panel of phages, we demonstrate that defense systems contribute substantially to defining phage host range and that overall phage resistance scales with the number of defense systems in the bacterial genome. We show that many individual defense systems target specific phage genera and that defense systems with complementary phage specificities co-occur in *P. aeruginosa* genomes likely to provide benefits in phage-diverse environments. Overall, we show that phage-resistant phenotypes of *P. aeruginosa* with at least 19 phage defense systems exist in the populations of clinical, antibiotic-resistant *P. aeruginosa* strains.

INTRODUCTION

Bacteriophage predation imposes a strong evolutionary pressure on bacteria to evolve mechanisms to defend against phage infection (*1*). These defense mechanisms include modification of cell surface receptors (*2*, *3*) and intracellular defenses (*4*–*6*) such as CRISPR-Cas (*7*, *8*) and restriction-modification (RM) (*9*, *10*).

More recently, dozens of previously unknown anti-phage immune systems have been found. In most instances, they were identified on the basis of the observation that immune systems often cluster in defense islands (*11*–*16*). The presence and composition of these defense islands vary among individual strains (*4*, *15*, *17*) and strongly contribute to phage-host coevolution in natural populations (*1*). The presence of multiple variable defense systems in bacterial genomes raises the important question of how these immune systems affect the overall phage resistance of bacterial pathogens.

To address this question, we assembled a set of 32 clinical, antibiotic-resistant *Pseudomonas aeruginosa* strains and compiled a custom panel of 28 phages from 12 phylogenetic groups. We then analyzed phage infectivity and adsorption of the strains across the panel. This revealed that intracellular phage defense mechanisms are an important determinant of the phage susceptibility of *P. aeruginosa* and that strains rich in phage defense systems are inherently more resistant to phage infection. Five strains contained a large number (13 to 19) of anti-phage defense systems and displayed an extended phage-resistant phenotype, in addition to having an extended drug-resistant phenotype. Our data further revealed that defense systems can be specific to certain phage families and that the activity of these individual defense systems in model strains can often predict the resistance of clinical strains to the same phages. In addition, we have found that some combinations of defense systems with complementary phage specificity often co-occur in *P. aeruginosa* genomes and may provide phage defense with broader phage specificity. Overall, our findings have implications for our understanding of phage defense and potentially for the development of phage-based antibacterial therapeutics, as antibiotic-resistant strains with extended phage-resistant phenotypes are present in clinical settings.

RESULTS

Defense systems are abundant and diverse in clinical *P. aeruginosa* strains

We selected a set of 32 antibiotic-resistant clinical strains covering the diversity of defense systems in the *P. aeruginosa* species as a whole. The *P. aeruginosa* genomes from the RefSeq database carry 71% (119 of 167) of the known defense system subtypes (Fig. 1A and table S1), which is in line with recent observations that *P. aeruginosa* has a diverse arsenal of anti-phage defense (*17*). The defense systems found in the RefSeq genomes resembled the defense arsenal in our clinical isolates (Fig. 1, B and C, and table S2), and the number of defense systems per genome ranged between 1 and 19 systems for both datasets (fig. S1, D and E). In addition, we assessed the phylogenetic distribution of our collection using a maximum likelihood analysis of the core genes using Parsnp (*18*), which revealed the distribution of the clinical isolates across the two main phylogroups, with 23 strains in the largest phylogeny group 1 and 9 strains in phylogeny group 2 (fig. S1). We found that the RefSeq genomes belonging to phylogeny group 2 carried a slightly higher number of defense systems compared to those of phylogeny group 1 (median phylogenetic group 1 = 7, median phylogenetic group 2 = 9, $P = 0.0004$), but these differences are not observed in the strains present in our collection ($P = 0.612$) (fig. S1). Overall, we demonstrate that *P. aeruginosa* genomes encode multiple different anti-phage defense systems and establish that our collection of clinical isolates is phylogenetically diverse and covers the range of defense systems both in types and numbers per strain as observed in *P. aeruginosa* as a whole.

[1]Department of Bionanoscience, Delft University of Technology, 2629 HZ Delft, Netherlands. [2]Kavli Institute of Nanoscience, Delft University of Technology, 2629 HZ Delft, Netherlands. [3]Medical Microbiology, University Medical Center Utrecht, Utrecht University, 3584 CX Utrecht, Netherlands. [4]School of Biological Sciences, University of Southampton, SO17 1BJ Southampton, UK.
*Corresponding author. Email: stanbrouns@gmail.com
†These authors contributed equally to this work.

Phage resistance correlates with the number of defense systems

To obtain a relevant panel of phages for these clinical isolates, we used a subset of 22 *P. aeruginosa* strains as hosts to enrich and isolate different phages from sewage water. We obtained a total of 27 phages (table S3), consisting of *Caudoviricetes* [double-stranded DNA (dsDNA) tailed phages], including 13 podophages (5 *Autographiviridae*, 3 *Bruynoghevirus*, 1 *Schitoviridae*, 1 *Zobellviridae*, and 3 unassigned phages), 4 siphophages (1 *Samunavirus*, 1 *Casadabanvirus*, 1 *Mesyanzhinovviridae*, and 1 *Detrevirus*), and 10 myophages [9 *Pbunavirus* and 1 *Phikzvirus*, a Jumbo myophage related to nucleus-forming *Pseudomonas* phage phiKZ (*19*)]. To broaden the diversity of our phage panel beyond dsDNA phages, we additionally included *Fiersviridae* PP7 [single-stranded RNA (ssRNA) phage]. We then used vConTACT2 (*20*) to assess the taxonomic diversity of our phage panel and found that it represents 9 out of the 16 phage clusters observed in *P. aeruginosa* phages overall, thus indicating a diverse representation of phages (fig. S2). A complete overview of the diversity within phage families and genera in our panel can be found in fig. S3.

To determine the effect of the defense systems on the susceptibility of the clinical strains to our panel of phages, we first assessed the ability of the phages to infect the strains or to only adsorb to their cell surface without infecting them. Out of a total of 924 phage-host combinations (28 phages times 33 hosts, including PAO1), 630 phage-host combinations did not result in infection (Fig. 2A). We hypothesize the noninfected phenotype can occur in two ways: either the phage fails to adsorb to the cell surface (i.e., no receptor) or phage propagation is unsuccessful, possibly due to anti-phage defense. On the basis of adsorption assay data, we found that a large proportion out of the 630 noninfection cases showed adsorption. More precisely, 68% (429) of the phage-host combinations showing no infection exhibited adsorption when considering an adsorption threshold of 50% (Fig. 2A), and 32% (201) when adopting a more

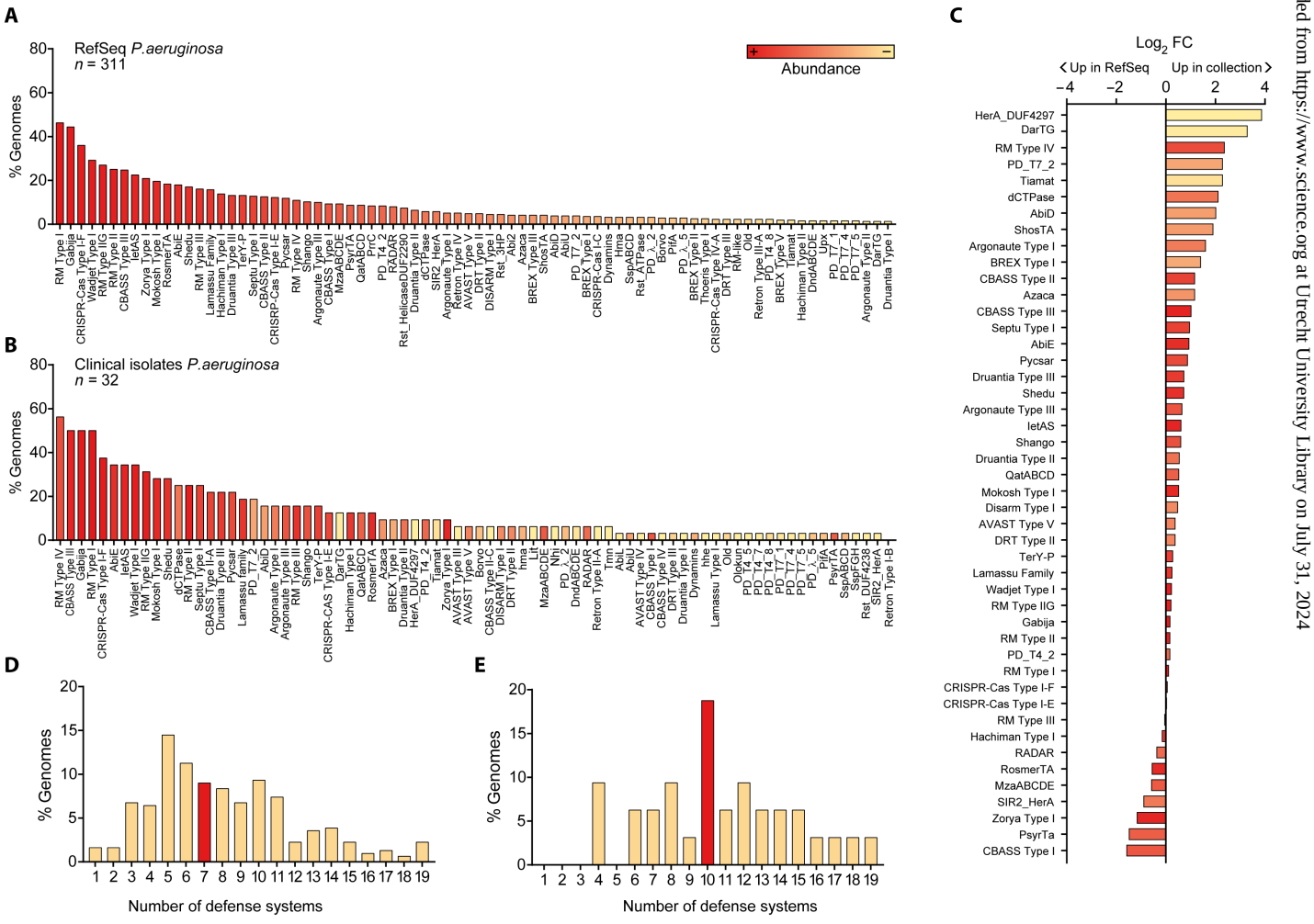

Fig. 1. Defense systems are abundant and diverse in *P. aeruginosa* strains. (**A**) Diversity of defense systems (DS) found in the genomes of 311 *P. aeruginosa* strains from the RefSeq database, organized and colored in a gradient from most (left) to least (right) abundant. Only the most prevalent DS are shown (see table S1 for the full list of DS). (**B**) Diversity of DS found in the genomes of 32 clinical isolates of *P. aeruginosa* from our collection. Systems are organized from most (left) to least (right) prevalent and colored according to the abundance in (A). All DS found in the clinical strains are shown. (**C**) Fold change (FC) of defense system abundance in our collection of clinical strains relative to the RefSeq strains. (**D**) Number of DS per genome in *P. aeruginosa* strains from the RefSeq database. (**E**) Number of DS per genome in *P. aeruginosa* strains from our collection of clinical isolates. For (D) and (E), the median number of DS is shown in red.

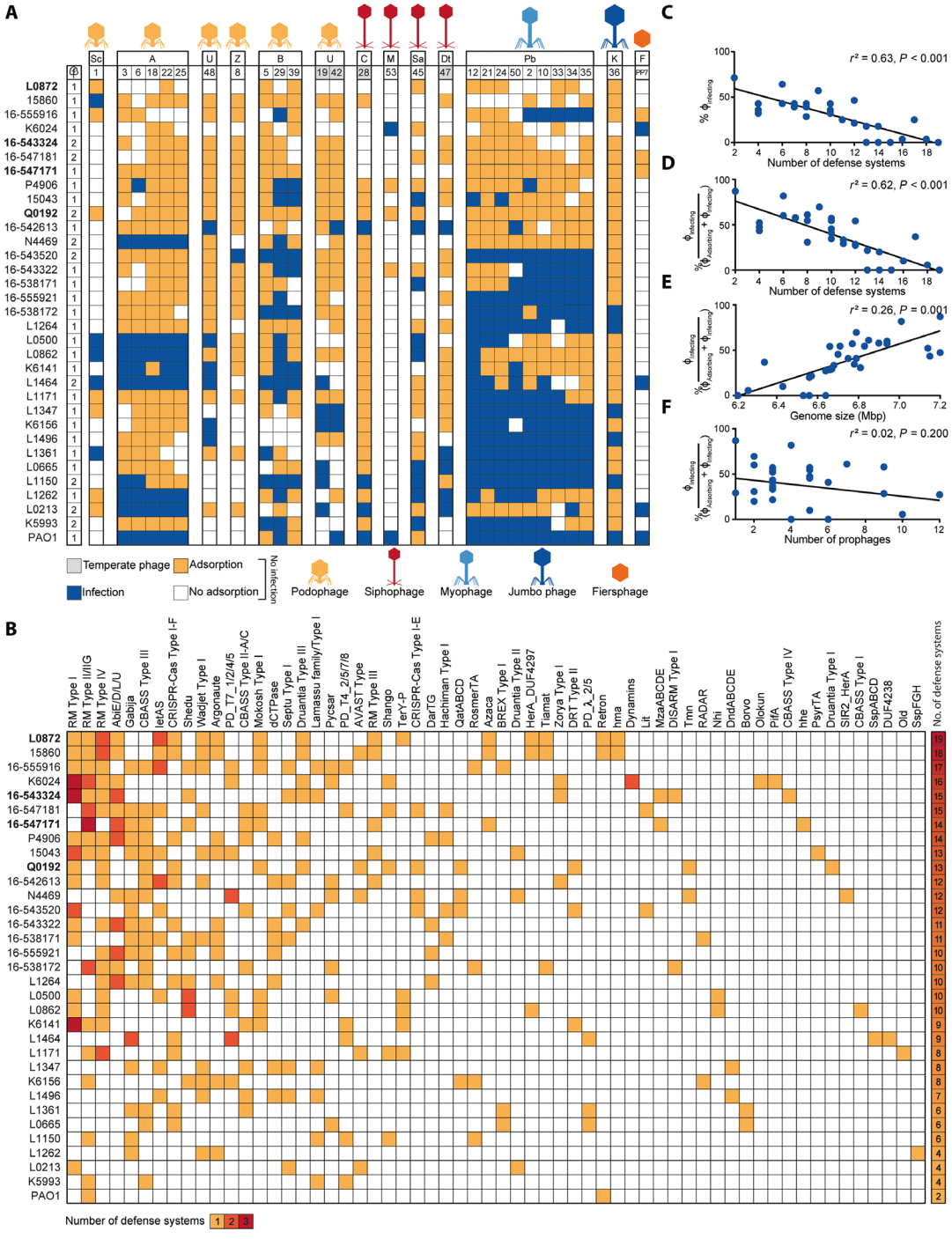

Fig. 2. Innate and adaptive defense systems correlate with phage resistance. (**A**) Host range of phages against 32 *P. aeruginosa* clinical isolates and strain PAO1. Phages are clustered by phylogeny (table S3). Phage-bacteria interactions are depicted as infection (blue), adsorption (>50%) but no infection (orange), or no interaction (white). Letters above the phage numbers indicate family or genus (for phages unassigned to a family): A, *Autographiviridae*; B, *Bruynoghevirus*; C, *Casadabanvirus*; Dt, *Detrevirus*; F, Fiersviridae; K, *Phikzvirus*; M, *Mesyanzhinovviridae*; Pb, *Pbunavirus*; Sa, *Samunavirus*; Sc, *Schitoviridae*; Z, *Zobellviridae*; U, unassigned. Strains not infected by phages in our panel are highlighted in bold. (**B**) DS found in the *P. aeruginosa* clinical isolates. The number of instances of each defense system type per strain is indicated in yellow, orange, or red for 1, 2, or 3, respectively. The total number of DS found per strain is indicated in a heatmap bar on the right. A complete list of the DS found in the clinical isolates can be found in table S2. (**C**) Linear regression analysis of how a number of DS found in the *P. aeruginosa* clinical isolates and PAO1 correlate with the levels of phage resistance, i.e., phages that could not adsorb and that adsorbed but failed to establish a productive infection. (**D**) Linear regression analysis of how a number of DS correlate with the levels of phage resistance calculated as the percentage of adsorbing phages that can establish a productive infection [% $\phi_{Infecting}/(\phi_{Adsorbing} + \phi_{Infecting})$]. (**E**) Linear regression analysis of how genome size correlates with phages that can establish a productive infection. (**F**) Linear regression analysis of how the number of prophages correlates with phages that can establish a productive infection. In (C) to (F), r^2 represents R-squared, a goodness-of-fit measure for the linear regression models.

conservative threshold of 90% (fig. S4A). These results indicate internal defense mechanisms could play a role in preventing infection in a substantial fraction of strains where no infection was observed. We ruled out the possibility of temperate phages (ϕPa19, ϕPa28, ϕPa42, and ϕPa47) integrating into the bacterial genome as the cause of instances where adsorption occurred but no infection, based on sequencing analysis of bacterial strains following phage infection, which showed no evidence of integrated phages (sequencing data available on the associated GitHub).

We observed that some of the *P. aeruginosa* strains (L0872, Q0192, 16-543324, and 16-547171), which encode more defense systems than average, exhibited complete resistance to our phage panel (i.e., no phage could establish productive infection despite adsorbing to these strains in many cases) (Fig. 2, A and B). Therefore, we questioned which factor is the main driver of phage resistance among (i) the number of defense systems, (ii) genome size, and (iii) number of prophages (*1*). To assess this, we performed a multiple linear regression analysis including these factors, which showed that defense systems are the only relevant indicator of phage resistance {$r^2 = 0.63$ and $P < 0.001$ for correlation with % infecting phages; $r^2 = 0.62$ and $P < 0.001$ for correlation with % adsorbing phages that can establish a productive infection [% $\phi_{Infecting}$/($\phi_{Adsorbing} + \phi_{Infecting}$)]} (Fig. 2, C to F, and fig. S4, B to E). The correlation between defense systems and phage resistance was reduced but remained significant when considering a conservative adsorption threshold of 90% ($r^2 = 0.35$ and $P < 0.001$) (fig. S4, F to H), or when only one representative phage per family or genus was included (number of defense systems $r^2 = 0.48$ and $P < 0.001$; genome size $r^2 = 0.11$ and $P = 0.033$; number of prophages $r^2 = -0.02$ and $P = 0.6256$) (fig. S4, I to L). Although the number of prophages did not show a significant correlation with phage resistance, we did observe mechanisms of superinfection exclusion (*21*) for strains L1361 and L1496, which contain one prophage each that likely provides protection against closely related temperate phages ϕPa47 (100% pident, 100% coverage) and ϕPa42 (100% pident, 89% coverage), respectively.

Overall, our findings suggest that the number of defense systems in *P. aeruginosa* is associated with phage resistance. This observation is best exemplified by the five *P. aeruginosa* strains (L0872, 16-543324, 16-547171, 16-547181, and Q0192) with 13 to 19 defense systems (Fig. 2, A and B) that were found to be resistant to the complete phage panel and to our attempts of phage isolation using wastewater from different sources. In summary, we show that phage-resistant strains of *P. aeruginosa* have accumulated phage defense systems in their genome, suggesting that phage defense systems could be a contributing factor to the phage sensitivity of the host.

Adaptive immunity targets temperate phages

Half (16 of 32) of the clinical strains contain adaptive immune systems in the form of CRISPR-Cas Type I-F (12 strains) and Type I-E (4 strains). To investigate the contribution of CRISPR-Cas to phage resistance, we identified all spacers targeting our phage panel and assessed their potential effect on the phage host range. We detected 70 spacers (43 unique) across 16 strains matching our phage panel (fig. S5A), among which 54 are predicted to be interference-proficient [i.e., spacers with matching protospacer adjacent motif (PAM) and protospacer] and 16 priming-proficient [i.e., spacers with $a \pm 1$ slipped PAM (*22*) or up to 5 protospacer mutations (table S4) (*23*, *24*)]. The majority of the spacers (65) originate from CRISPR-Cas Type I-F systems, with only five spacers from CRISPR-Cas Type I-E systems (strains 15-547181, N4469, and 15043, all targeting ϕPa28). Sixty-six of the 70 spacers target temperate phages (ϕPa19, ϕPa28, ϕPa42, and ϕPa47), and only four spacers match a virulent phage (ϕPa8). This is in line with previous findings that spacers of *P. aeruginosa* mostly match temperate phages (*25*). Our data on phage infection and adsorption reveal that in 83% (25 of 30) of cases with matching I-E (4 of 4) and I-F (21 of 26) spacers, the targeted phage was unable to infect (fig. S5A). Out of the five cases where the protective effects of matching spacers were not observed (fig. S5A), one was linked to the presence of an Acr (ϕPa42 infecting 16-542613) (fig. S5B and table S5).

Overall, our results suggest that CRISPR-Cas Type I-E and I-F may contribute to resistance of the clinical strains against temperate phages but play a minor role against the vast majority of virulent phages in the panel because they are not targeted. Although the catalog of spacers may evolve through CRISPR adaptation, the current set of spacers alone does not explain the observed infection profiles.

Innate defense systems provide anti-phage activity against specific phage families

To understand the contribution of individual innate defense systems to broad-spectrum phage immunity, we inserted 14 individual defense systems (fig. S6A) from *P. aeruginosa* clinical isolates into the low-copy plasmid pUCP20 (*26*), under their native promoters. The plasmids were introduced into *P. aeruginosa* strain PAO1, which is infected by 18 phages of our panel. We validated that the defense systems represent no obvious burden or toxicity to cell growth (Kruskal-Wallis test followed by Dunn's post hoc test; fig. S6B) and subsequently assessed the defense-containing PAO1 strains for changes in phage susceptibility in solid and liquid media using efficiency of plating assays (EOP; Fig. 3, A and B) and infection dynamics assays to measure phage titer over time (fig. S7). We further monitored bacterial survival upon phage exposure using culture collapse assays (Fig. 3C and fig. S8).

The EOP (Fig. 3B) and infection dynamics (fig. S7) assays show that 9 out of 14 defense systems exhibit activity against the phage panel. Of these, most (five) are active against at least two phage families or genera. For example, Zorya Type I is active against podo *Bruynoghevirus*, sipho *Casadabanvirus*, and *Fiersviridae*. QatABCD and RADAR are both strong defenses against myo *Pbunavirus* and target members of different families of siphophages (*Casadabanvirus* and *Mesyanzhinovviridae*, respectively). CBASS Type III-C displays the broadest protection in our set, acting against podo *Autographiviridae*, sipho *Mesyanzhinovviridae* and *Casadabanvirus*, myo *Pbunavirus*, and Jumbo *PhiKZvirus*. This suggests that these defense systems use sensing and targeting mechanisms that rely on phage features shared among different families, such as proteins (*27*–*30*) or phage-induced changes in host metabolism (*31*) and cell integrity (*32*, *33*) or that their effector is activated by other cellular responses, such as a general stress response. Zorya Type I is the only defense system among those tested that prevents infection of ssRNA phage PP7 (*Fiersviridae*), suggesting also that the effector may be activated by general cellular responses to phage infection. In addition, CBASS Type III-C and AVAST Type V systems provide robust (>10^5-fold) protection against infection by phiKZ-like, nucleus-forming Jumbo phage

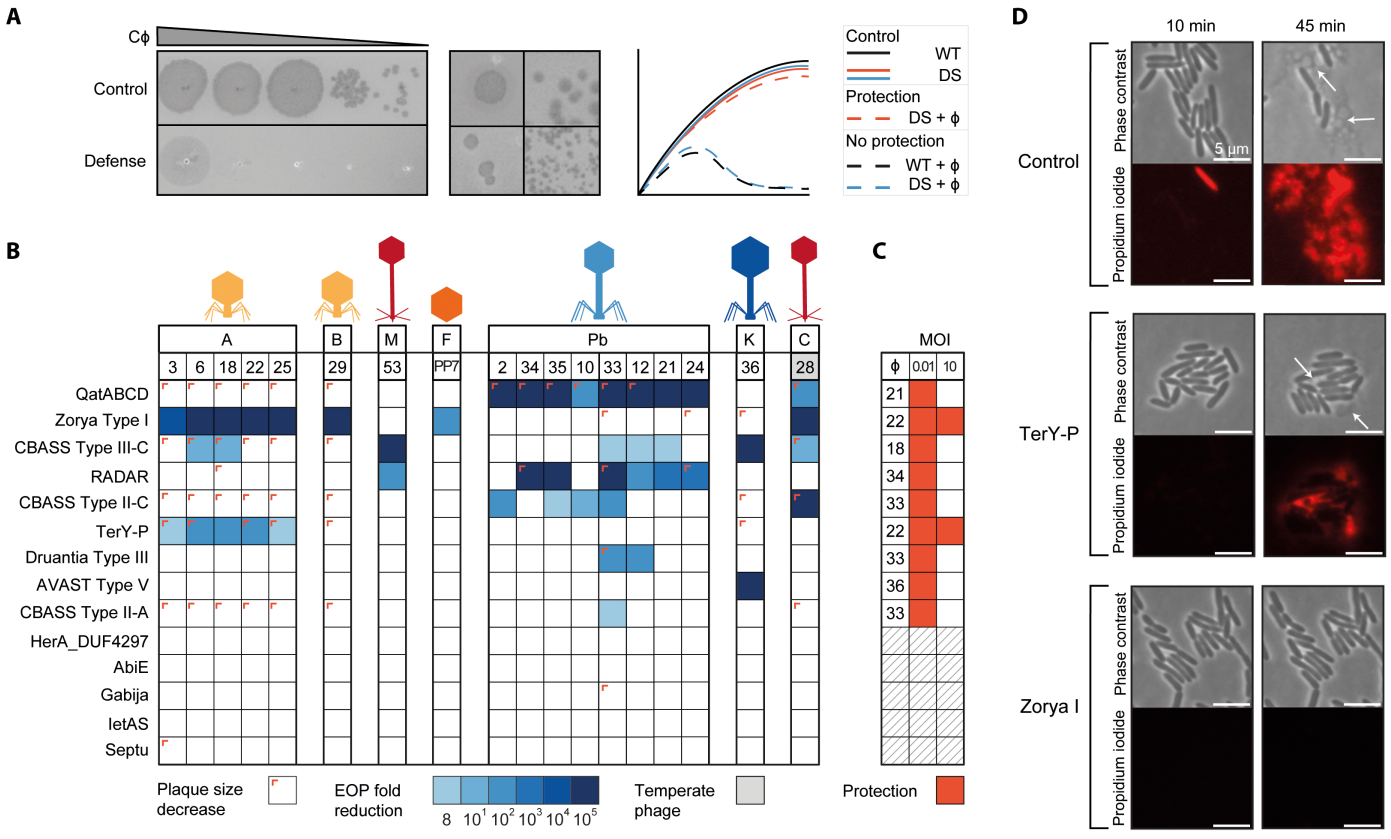

Fig. 3. Defense systems provide genera-specific anti-phage activity. (**A**) Representation of the assays used to assess the effect of individual DS on phage infectivity. Left: An example of fold decrease in ϕPa33 phage infectivity caused by the defense system QatABCD. Middle: Examples of phage plaque size decrease observed for *Autographiviridae* ϕPa3 and *Casadabanvirus* ϕPa28 with QatABCD cells. Right: Illustrations of growth curves obtained from liquid culture collapse assays for control strains (wild type, WT) and strains containing individual DS with and without phage infection, showing cases of protection (orange) and no protection (blue). (**B**) Efficiency of plating (EOP) of phages in PAO1 containing individual DS. EOP was determined as the fold decrease of phage titer in the strain with the defense system compared to the titer obtained in the strain without the defense system. Plaque size reductions are indicated as a colored corner. (**C**) Liquid culture collapse assays of PAO1 containing individual DS infected with phages, as compared to a control (WT) without a defense system. Results are shown as a summary of the effects observed when infecting the cultures with a multiplicity of infection (MOI) of 10 or 0.01. A protective effect is represented as dark orange. The absorbance values at 600 nm of representative phage-host combinations are shown in fig. S8. (**D**) Time-lapse phase contrast and fluorescence images of PAO1 cells containing individual DS infected with phage ϕPa25. Cells were stained with propidium iodide to visualize the permeabilization of the cell membrane due to cell death. TerY-P and Zorya Type I cells survive phage infection, although some cell death is still observed for TerY-P, consistent with the EOP results in (B).

ϕPa36 (Fig. 3, B and C). Both systems have been reported to act via altruistic cell death upon sensing a specific phage protein (*27, 28, 34*), a strategy that [like RNA-targeting CRISPR-Cas systems (*35*)] circumvents the nuclear shell defense used by Jumbo phages to overcome DNA-targeting defense systems (*36*–*38*). The bacterial culture collapse assays provided additional information about the protective effect of the defense systems in liquid culture. TerY-P and Zorya Type I protect the cell population at both low and high phage multiplicity of infection (MOI) (Fig. 3C and fig. S8), and most cells survive infection monitored using microscopy with propidium iodide as an indicator of membrane permeability and cell death (Fig. 3D). For QatABCD, RADAR, Druantia Type III, AVAST Type V, CBASS Type III-C, II-A, and II-C, a culture collapse is observed when the phage is introduced at high MOI. In summary, our findings indicate that some individual defense systems display phage-targeting activity against specific phage families, while others are broader and target a few families. While the majority of the defense systems could provide protection against phages at low concentrations, only two were efficient against phages at high densities.

Linking native infection profiles with protection patterns of individual systems

To understand the overall phage protection observed in genetically inaccessible clinical strains (Fig. 2) in relation to the effect of individual phage defense systems (Fig. 3), we initially assessed the phage infectivity levels in these strains using EOP assays (fig. S9A). We then compared the phage susceptibility profiles of the clinical strains with those of PAO1 strains equipped with a single defense system. Our findings indicate that in 84% of the cases, the phage susceptibility profile of the clinical strains aligns with the expected profile (fig. S9B). This is especially evident for Zorya Type I, TerY-P, Druantia Type III, AVAST Type V, and CBASS Type II-A. The most notable disparity in the results was observed for RADAR and CBASS Type

II-C, as they were providing protection against *Pbunavirus* in PAO1 and not in the clinical strains (ϕPa34 and ϕPa35 for RADAR; ϕPa2, ϕPa10, ϕPa33, and ϕPa35 for CBASS Type II-C).

To assess whether known phage-encoded anti-defenses affect the phage infectivity profile of the clinical strains, we searched phage genomes for anti-defense genes including anti-RM (*39*–*41*), anti-CBASS (*28, 42*), anti-Pycsar (*42*), anti–TIR-STING (*43*), and anti-AVAST (*27*) proteins (fig. S5B and table S5). We focus here specifically on the anti-defenses against the defense systems introduced in PAO1, which include anti-CBASS and anti-AVAST. Our search identified one phage-encoded anti-defense gene, an anti-CBASS Type II (*acbII*) in phage ϕPa48. The *acbII* gene inhibited only the activity of CBASS type II-C in PAO1 (fig. S5C), but its impact on the phage host range in the clinical strains is not clear since ϕPa48 can only infect one (L1496) out of the two strains that carry CBASS Type II-C (Fig. 2, A and B, and table S2). This outcome is possibly due to other defense systems that target ϕPa48 in this strain.

Next, we focused on the anti-defense genes present within the bacterial genomes. We postulated that an increased quantity of these anti-defense genes within a strain might lead to increased susceptibility to our phage panel. To test this hypothesis, we performed a multiple linear regression analysis. Unexpectedly, we observed that the presence of known anti-defenses does not have a detrimental effect on the phage resistance of the host ($r = 0.36$, $r^2 = 0.13$, $P = 0.04$). This may be linked to the regulation of anti-defense gene expression in the host, as observed for Aca repression of Acrs (*44*). Among the anti-defense genes identified in the strains (fig. S5B), only *acbII* was found to target a defense system that was tested in PAO1. The *acbII* gene was found in strains L1347 and 16-547171, which carry the CBASS Type II-C and II-A systems, respectively, and here, it is in line with the expected infection phenotype in four out of six cases (Fig. 2A and fig. S5B). The suppression of *acbII* expression or the presence of other defense systems may be the reasons why in two cases the bacteria can resist phages despite having an anti-defense gene. Overall, our findings underscore the intricate nature of phage susceptibility in natural settings, which is likely influenced by the interaction between different defense and anti-defense mechanisms present in both the strain and the phage.

Co-occurrence of defense systems with complementary specificities

On the basis of the observation that some defense systems provide distinct genera-specific anti-phage activities (Fig. 3), we hypothesized that combinations of defense systems may be advantageous for cells by providing a wider protective range and would be a conserved feature in bacterial genomes to efficiently achieve broader antiviral specificity. To test this hypothesis, we assessed the co-occurrence (i.e., the presence in the same genome) of defense systems in *P. aeruginosa* genomes in the RefSeq database ($n = 311$) while taking phylogeny into account (*45*).

We found multiple defense system co-occurrences [147 out of 1317 (11%) combinations tested, Bonferroni-corrected binomial exact test statistic with $P < 0.01$], seven of which involved defense systems with anti-phage activity in this study (table S6). Of these, six combinations have complementary phage specificity, including: (i) Druantia Type III (*Pbunavirus*) and TerY-P (*Autographiviridae*), (ii) Druantia Type III (Pbunavirus) and Zorya Type I (*Autographiviridae*, *Bruynoghevirus*, *Casadabanvirus*, and *Fiersviridae*), (iii) Druantia Type III (Pbunavirus) and AVAST Type V (*Phikzvirus*), (iv) AVAST Type V (*Phikzvirus*) and QatABCD (*Casadabanvirus* and *Pbunavirus*), (v) AVAST Type V (Phikzvirus) and Zorya Type I (*Autographiviridae*, *Bruynoghevirus*, *Casadabanvirus*, and *Fiersviridae*), and (vi) TerY-P (*Autographiviridae*) with CBASS Type II (*Casadabanvirus* and *Pbunavirus*). Druantia Type III and CBASS Type II have overlapping specificity for *Pbunavirus*, with CBASS Type II adding specificity to *Casadabanvirus*. A binomial test indicates that complementary defense system combinations co-occurred significantly more often than expected [Binomial test: $n = 7$, $x = 6$, $P = 26/56$, $P(X \geq x) = 0.042$]. Overall, our analysis suggests that defense systems with complementary anti-phage activity co-occur at a probability higher than by chance in *P. aeruginosa* genomes and could provide an advantage for bacterial survival in phage-diverse environments.

DISCUSSION

Bacterial strains carry numerous distinct phage defense systems in their genomes (*17*). We found that *P. aeruginosa* strains carry at least 71% of all currently known defense systems, making this species a versatile bacterial model to study phage immunology. Using a diverse set of clinical isolates of *P. aeruginosa*, we observe that strains that have accumulated defense systems in their genome display broad and robust immunity against phage infection.

By testing the activity of 14 defense systems against our phage panel, we observed that the majority (seven out of nine active systems) of the defense systems tested in PAO1 are capable of protecting the cell population at low phage concentration (MOI < 1), but not at high concentration (MOI ≥ 1). This phenotype could be caused by the defense system being overwhelmed at high phage concentration or by death or dormancy of the infected cell (*46*) which serves as a means of protecting the cell population through kin selection. In addition, we show that defense systems have anti-phage specificity that is often linked to a few phage families or genera, suggesting that these defense systems use a more general sensing mechanism or that their effector is activated by other cellular responses. This is especially evident for Zorya Type I and CBASS Type III-C, which were effective against multiple distinct phage families. While Zorya remains largely uncharacterized, the current knowledge of CBASS activation suggests a variety of phage sensing strategies, including the recognition of peptides (HORMA domain) and dsDNA binding (cyclase) in *Escherichia coli* CBASS Type III-C (*34*), binding of structured phage RNA in *Staphylococcus schleiferi* CBASS Type I-B (*47*), and phage-driven depletion of folate-like molecules in *Vibrio cholerae* CBASS Type II (*48*).

We found that several pairs of the tested defense systems, which exhibit complementary anti-phage specificities, co-occur in *P. aeruginosa* strains. We expect that these combinations of defense systems could provide a broader range of phage protection through the complementary phage specificities of each individual defense system. The complementary activities of naturally co-occurring defense systems have also been found to enable resuscitation from defense system-induced bacterial dormancy (RM and CRISPR-Cas) (*49*) and to prevent plasmid dissemination in *V. cholerae* El Tor strains (DdmABC and DdmDE) (*50*), the latter proposing that defense system cooperation might play a role in bacterial pathogenicity.

The strong correlation found between a number of defense systems and phage resistance further indicates that multiple defense system combinations are beneficial to cover the whole range of predating phages. The importance of the number of defense systems in determining phage resistance is further evidenced by the high levels of phage resistance of five of our clinical isolates that encode between 13 and 19 defense systems. Attempts to isolate phages from diverse wastewater samples against defense-rich strains or to transform plasmid DNA proved more difficult, again pointing to the strains' inherent ability to defend well from incoming threats.

Our findings demonstrate the significance of the individual defense systems in predicting the susceptibility of *P. aeruginosa* strains to phages. However, factors such as genetic context, interactions among defense systems (*49, 51–53*), the presence of unknown defense systems, and anti-defense mechanisms will affect the final outcome of phage infection. Further research is required to enhance the predictive accuracy of genomic analysis, which could prove beneficial for ecological and evolutionary studies.

Together, our results show that while phage host range has traditionally been linked to receptor-associated factors (*54*), the number of defense systems is also a strong indicator of the susceptibility of cells to phage in *P. aeruginosa*. Naturally occurring *P. aeruginosa* clinical strains with a large number of defense systems show increased resistance to phages and may be selected for more widespread use of therapeutic phages. Therefore, monitoring the evolution and spread of phage-resistant clinical pathogens and selecting or engineering phages with anti-defense properties may become instrumental in combatting antimicrobial resistance using phage.

MATERIALS AND METHODS

Bacteria

A set of 22 clinical isolates of *P. aeruginosa* provided by University Medical Center Utrecht (UMCU) was used for phage isolation and 32 for characterization of the host range (table S2). The antibiotic susceptibility of the strains was established using the broth microdilution method outlined by EUCAST for determining the minimal inhibitory concentration and interpreted according to the EUCAST 2023 breakpoints (www.eucast.org). *E. coli* strain Dh5α was used to clone plasmid pUCP20 with individual defense systems. *P. aeruginosa* strains containing pUCP20 with individual defense systems were constructed from *P. aeruginosa* strain PAO1. All bacterial strains were grown at 37°C in lysogeny broth (LB) with 180 rpm shaking for liquid cultures or in LB agar (LBA) plates for solid cultures. Strains containing plasmid pUCP20 were grown in media supplemented with ampicillin (100 μg/ml; for *E. coli*) or carbenicillin (200 μg/ml; for *P. aeruginosa*).

Bacteriophages

Phages used in this study are described in table S3. All phages were isolated from sewage water. Approximately 1 ml of sewage sample was added to 20 ml of LB, inoculated with 100 μl of overnight cultures of each *P. aeruginosa* clinical isolate, and incubated overnight at 37°C with 180 rpm shaking. Samples were centrifuged at 3000*g* for 15 min and filter-sterilized (0.2-μm polyethersulfone). The phage-containing supernatant was serially diluted in LB and spotted onto double-layer agar (DLA) plates of the isolation strains for the detection of phages. Single plaques with distinct morphologies were picked with sterile toothpicks and spread with sterile paper strips onto fresh bacterial lawns. The procedure was repeated until a consistent plaque morphology was obtained. Phages from purified plaques were then produced in liquid media with their respective host, centrifuged, filter-sterilized, and stored as phage lysates at 4°C. For EOP and liquid infection assays (see below), phage stocks were obtained from lysates prepared on PAO1, and their concentration normalized to $\approx 1 \times 10^8$ plaque-forming units (pfu)/ml. Additional efforts were made to isolate phages for the *P. aeruginosa* clinical isolates that exhibited the highest phage resistance. This involved using sewage water from various sources and following the enrichment procedure outlined above, but with individual strains instead of mixtures.

Phage host range

Phages were 10-fold serially diluted in LB and spotted onto DLA plates containing each of the 32 *P. aeruginosa* clinical strains used for phage characterization (table S2). The plates were incubated overnight at 37°C and the phage plaques were observed to distinguish productive infection (lysis with individual phage plaques formed) from lysis from without (*55*) (lysis without individual phage plaques). EOP of phages in each clinical strain was determined by comparing phage titer to that obtained in PAO1 (for phages that infect this strain) or in the clinical strain with the highest phage titer (for phages that cannot infect PAO1).

Adsorption assays

Early-exponential cultures (optical density at 600 nm, $OD_{600} \approx 0.3$) of the *P. aeruginosa* clinical isolates were added in triplicates to the wells of 96-well plates. Phages were added to these cultures at an MOI of 0.01 and incubated at 37°C with 100 rpm shaking for 15 min. The plates were centrifuged and a sample of the supernatant was taken, 10-fold serially diluted, and plated onto DLA plates of PAO1 to determine the titer of phages that did not adsorb to the clinical strain. A control plate in which phages were added to LB was used to determine the total phage concentration. The concentration of adsorbed phages was determined by subtracting non-adsorbed phage concentration from the total phage concentration in the suspension. The percentage of adsorbed phages was calculated as the ratio between adsorbed phages and total phages. Phages were considered to adsorb when over half of their population on average adhered to the cells.

Extraction of phage DNA and bacterial DNA

Phage DNA was extracted using phenol-chloroform. For this, 5 ml of each phage lysate at $>10^9$ pfu/ml was treated with DNase I and RNase (1 μg/ml) for 30 min. EDTA, proteinase K, and SDS were added to the sample at final concentrations of 20 mM, 50 μg/ml, and 0.5%, respectively, and the samples were incubated at 56°C for 1 hour. The samples were then mixed with an equal volume of chloroform and centrifuged at 3000*g* for 10 min. The aqueous phase was recovered and the procedure was repeated sequentially with a 1:1 mixture of phenol:chloroform and with chloroform. The resulting aqueous phase was mixed with 0.1 volume of sodium acetate 3 M (pH 5) and 2.5 volumes of ice-cold absolute ethanol and incubated at −20°C overnight. The extracted DNA was pelleted at 14,000*g* for 15 min and washed in ice-cold 70% ethanol, before resuspending in ultrapure water. Bacterial genomic DNA was extracted using the GeneJET Genomic DNA Purification kit (Thermo Fisher Scientific).

The quality and quantity of extracted phage and bacterial DNA were estimated using a NanoPhotometer and a Qubit fluorometer, respectively.

Phage genome sequencing

For samples sequenced at Beijing Genomics Institute (BGI) (table S3), the phage genomic DNA was fragmented by Covaris 55 μl series ultrasonicator and used to construct DNA nanoball–based libraries by rolling circle replication. DNA was sequenced using the BGI MGISEQ-2000 platform (BGI Shenzhen, China) with a 100-nucleotide paired-end strategy, generating 4.6- to 19.2-Gb sequencing data for each sample. For phage samples sequenced in-house, phage DNA was fragmented by Covaris M220 Focused-ultrasonicator, and libraries were prepared using the NEBNext Ultra II DNA Library Prep Kit. Size distribution was checked on an Agilent D1000 Screen Tape System, and the libraries were pooled equally and spiked with approximately 5% of the PhiX control library. The pooled library was sequenced with an Illumina MiSeq using the MiSeq Reagent Nano Kit v2 (500 cycles). For samples sequenced at the Microbial Genome Sequencing Center (MiGS, Pittsburgh, PA, USA), sample libraries were prepared using the Illumina DNA Prep kit and IDT 10–base pair (bp) UDI indices and sequenced on an Illumina NextSeq 2000, producing 2 × 151 bp reads. Demultiplexing, quality control, and adapter trimming were performed with bcl-convert (v3.9.3). Reads obtained for all samples were assembled using Unicycler v0.5.0 (*56*). For samples sequenced in-house, the control PhiX was manually removed from the assembled contigs using Bandage (*57*).

Bacterial genome sequencing

For samples sequenced at BGI (table S2), the bacterial genome was fragmented by Covaris 55 μl series ultrasonicator and used to construct paired-end libraries with an insert size of 200 to 400 bp. Bacterial genomes were sequenced on the BGISEQ-500 (MGI, BGI-Shenzhen) platform, generating 1.4- to 2.0-Gb sequencing data for each sample with a sequencing depth >100×. Reads were checked for contamination using kraken2 (*58*) and only considered for further analysis if >90% of the reads were identified as *P. aeruginosa*. Quality control of the raw data was performed using FastQC (*59*) with default parameters. For samples sequenced at MiGS, sequencing was performed as described above for phages. Reads obtained for all samples were assembled using Unicycler and the assembly quality was assessed using assembly-stats.v1.0.1 (https://github.com/sanger-pathogens/assembly-stats) and BUSCO.v4 (*60*) (pseudomonodales_odb10), and the GC% was calculated using bioawk (https://github.com/lh3/bioawk). The sequencing depth was calculated using minimap2 (*61*) and SAMtools mpileup (*62, 63*).

Bacteria genome annotation and phylogenomics

Bacterial genomes of the clinical strains were annotated using Prodigal (*64*). The genomes were used to determine the multi-locus sequence type (MLST) of the strains using the PubMLST website (https://pubmlst.org/) (*65*) and the serotype using the *P. aeruginosa* serotyper PAst (https://github.com/Sandramses/PAst). A total of 311 complete *P. aeruginosa* genomes were downloaded from RefSeq in February 2022. A phylogenetic tree of the core genome of *P. aeruginosa* was constructed using Parsnp (*66*) with default parameters using *P. aeruginosa* strain PAO1 (NC_002516.2) as the reference genome. Parsnp aligns microbial genomes to identify both structural and point variations by searching for maximal unique matches to produce a core-genome alignment. Single-nucleotide polymorphisms in this core-genome alignment are filtered by Parsnp based on repetitive sequences, small locally collinear block size, poor alignment quality, poor base quality, and possible recombination events. The final alignment was given to FastTree2 for the construction of the phylogenetic tree. Phylogeny groups were determined as previously described (*18*). The number of complete prophages present in RefSeq and clinical strains was predicted with virsorter2 v2.2.4 (*67*), checkv v1.0.1 (*68*) (end_to_end with checkv-db-v1.0), and a second round of virsorter2 v2.2.4, following the protocol described in www.protocols.io/view/viral-sequence-identification-sop-with-virsorter2-5qpvoyqebg4o/v3. Superinfection exclusion was considered when the prophage and temperate phage shared a nucleotide similarity of pident >90% and coverage >85%.

Phage genome annotation, taxonomy, and phylogenomics

Phage genomes were annotated using the RAST server (*69*), the start of the phage genome was determined using PhageTerm (*70*), and partial genes were manually verified and removed. The phage lifestyle was predicted using PhageAI (*71*). Phages from our collection were classified taxonomically using GRAViTy (*72*). Phage diversity was evaluated using vConTACT2 (*20*) with the default settings and the ProkaryoticViralRefSeq94-Merged database, specifically selecting for *P. aeruginosa* phage genomes. The output of vConTACT2 was visualized in a circular layout using Cytoscape (*73*). Phages within the same family/genus were compared using clinker (*74*) for their similarity in gene structure and on sequence level using blastn (*75*).

Detection of defense systems in bacterial genomes

Defense systems were detected in the *P. aeruginosa* genomes of RefSeq and clinical isolates with PADLOC-DB v1.4.0 (*76*), DefenseFinder (*17*), and the Hidden Markov Models (HMMs) with completeness rules and thresholds as applied in (*77*). In addition, the representative sequences provided by Rousset *et al.* (*78*) were used to search for the defense system Detocs described in this work. Homology searches were performed via blastp (*75*) (>0.7 subject length/query length < 1.5; 0.7 > query coverage < 1.3; *e* value < 1×10^{-9}). Systems were considered complete when all genes were present without more than two genes in between. In case of discrepancies between the algorithms, we considered the output reporting the most hits. For PADLOC, we excluded defense systems of the "other" categories. For DefenseFinder, we excluded results of defense systems that were not discriminated into subtypes, e.g. BREX.

In addition, a manual search of the neighborhood of the defense systems identified by the algorithms led to the identification of a variant of the TerY-P system that contained all three genes and corresponding functional domains of the original system (*77*). The previously unidentified TerY-P sequences were used to search for this variant in the bacterial genomes using blastp with *e* value < 2.34×10^{-29} and pident > 30. Systems were considered complete when all genes were present with less than three genes in between.

Detection of CRISPR-Cas I-F and I-E spacers targeting phages from our collection

Spacers were detected in the bacterial genomes using CRISPRDetect (*79*) and were mapped to our phage collection using blastn (word size = 8; *e* value = 1; query coverage > 90; pident > 90;

no gaps; maximum of one mismatch allowed). The nontarget strand PAM (5′-CC for I-F; 5′-AAG for I-E) was manually checked, with $a + 1$ or -1 PAM slippage allowed for I-F (*22*). Spacers with a matching PAM and protospacer were categorized as interference-proficient, while spacers with a PAM slippage or up to five protospacer mutations (with correct PAM) were categorized as priming-proficient spacers.

Detection of anti-defense genes in bacteriophage and bacterial genomes

Acrs were detected using AcrFinder (*80*). For the detection of anti-RM [*ardA* (*39*), *klcA* (*40*), *ardB*, *ocyA*, *ocr*, *darA*, and *darB* (*41*)], anti-CBASS Type I (*acb1*) (*42*), anti-CBASS Type II (*acbII*) (*28*), anti-Pycsar (*apyc*) (*42*), anti–TIR-STING (*43*), and anti-AVAST (*lidtsur-6*, *lidtsur-17*, *forsur-7*, *penshu1-7*, *usur-3*, *smaarsur-6*, and *mellemsur-6*) (*27*) genes, we first searched for *P. aeruginosa* homologs using PSI-BLAST (*81*) (maximum of three runs with 500 sequences; coverage > 60%, pident > 20%). Homolog functionality was checked using HMMer (*82*) and HHpred (*83*). *P. aeruginosa* homologs were only found for anti-genes *acb1* and *acbII*. These homologs were searched for in our phage and bacterial genomes with the use of blastp (*e* value < 10^{-8}; pident > 30; coverage > 60%; 2.0 < subject length/query length > 0.5). For genes with no *P. aeruginosa* homologs, we created an HMM from the multiple alignment file obtained from the PSI-BLAST search above, using hmmbuild v3.3.2 (*82*) with default settings. These HMMs were used to search for the anti-defense genes in our phage and bacterial collections (*e* value < 10^{-6}). All hits obtained were checked for the presence of the expected functional domains by HMMer and HHpred.

Co-occurrence of defense systems

Coinfinder (*45*) was used for detecting the co-occurrence of defense systems in the *P. aeruginosa* genomes of the RefSeq database, using the Parsnp (*65*) phylogenetic tree as input. We calculated the percentage of overlapping (for at least one phage) and complementary combinations in our set of tested defense systems. For this analysis, we combined the two CBASS type II subtypes (A and C) since our co-occurrence analysis in the RefSeq database was performed on the combination of all CBASS type II subtypes. A binomial test was then performed to test whether the frequency of co-occurring complementary defense systems deviated from the expected.

Cloning of defense systems in PAO1

Defense systems were amplified from *P. aeruginosa* strains using the primers indicated in table S7 with Q5 DNA Polymerase (New England Biolabs), in reactions that added regions of homology to plasmid pUCP20. PCR products were run on 1% agarose gels and bands of the desired size were excised and cleaned using the Zymoclean Gel DNA Recovery Kit. Plasmid pUCP20 (pEmpty; table S8) was digested with BamHI and EcoRI, treated with FastAP (Thermo Fisher Scientific), and cleaned with the Zymo DNA Clean & Concentrator Kit. Each defense system was cloned into pEmpty using the NEBuilder HiFi DNA Assembly Master Mix and transformed into chemically competent NEB 5-alpha Competent *E. coli* following the manufacturer's instructions. Plasmids were extracted using the GeneJET Plasmid Miniprep kit, confirmed by sequencing (Macrogen; primers in table S7), and electroporated into PAO1 as previously described (*84*). Briefly, an overnight culture of PAO1 was centrifuged at 16,000*g* for 2 min at room temperature, and the pellet was washed twice and resuspended in 300 mM sucrose. The suspension was mixed with 100 to 500 ng of plasmid DNA and electroporated at 2.5 kV in a 2-mm gap electroporation cuvette. Cells were recovered in LB for 1 to 2 hours at 37°C and plated in LBA plates supplemented with carbenicillin (200 μg/ml).

Cloning of anti-defense gene *acbII* into PAO1

Gene *acbII* was amplified from øPa48 using the primers indicated in table S7 with Q5 DNA polymerase, in reactions that added regions of homology to plasmid pSTDesR (*85*). Plasmid pSTDesR was amplified with the primers indicated in table S7 and digested with DpnI (New England Biolabs) for 1 hour at 37°C. PCR products were run on 1% agarose gels and bands of the desired size were excised and cleaned using the Zymoclean Gel DNA Recovery Kit. Gene *abcII* was cloned into the amplified pSTDesR using the NEBuilder HiFi DNA Assembly Master Mix and transformed into chemically competent NEB 5-alpha Competent *E. coli* following the manufacturer's instructions. Plasmids were extracted using the GeneJET Plasmid Miniprep kit, confirmed by sequencing (Macrogen; primers in table S7), and electroporated into PAO1.

Efficiency of plating

The phage stocks (10^8 pfu/ml) were 10-fold serially diluted in LB and the dilutions were spotted onto DLA plates of PAO1 or DLA + carbenicillin plates of PAO1 with pEmpty or PAO1 with individual defense systems following the small plaque drop assay (*86*). The phage dilution that resulted in countable phage plaques was used in double-layer overlay plaque assays (*87*) with PAO1, PAO1 with pEmpty, or PAO1 with the defense systems. The anti-phage activity of the systems was determined as the fold reduction in phage plaques in comparison to the number of plaques obtained in the PAO1:pEmpty control. The diameter of the phage plaques was measured to determine differences in plaque size caused by the defense systems.

Infection dynamics of phage-infected cultures

Bacterial cultures of PAO1 with pEmpty or with individual defense systems at an $OD_{600} \approx 0.1$ were infected with phage at an MOI < 1. The cultures were incubated at 37°C with rocking, and samples were taken at 0, 2, 4, and 6 hours to measure phage concentration. The sample was centrifuged at 3000*g* for 5 min, and the phage-containing supernatant was 10-fold serially diluted and spotted onto DLA plates of PAO1 to estimate phage concentration.

Liquid culture collapse assays

Overnight-grown bacteria were diluted to an OD_{600} of approximately 0.1 in LB media. The cell suspension was distributed into the wells of 96-well plates, and phages were added at MOIs of 10, 0.1, 0.01, and 0.001. Assays were performed in triplicates. The plates were incubated at 37°C in an Epoch2 microplate spectrophotometer (BioTek) for OD_{600} measurements every 10 min for 24 hours, with double orbital shaking. The growth rate of uninfected cells carrying the empty plasmid and each defense system was determined by comparing the OD measurement at the beginning of the log phase (OD1 at 3 hours) to that at the end (OD2 at 6 hours), using the natural log: $\ln[(OD2 - OD1)/(t2 - t1)]$. The growth rate of the cells carrying defense systems was compared to that of the cells carrying an empty plasmid using the Kruskal-Wallis test followed by Dunn's post hoc test.

Sequencing of phage-infected bacterial strains

The genomic DNA of bacterial strains infected with phage for 6 hours was extracted using the GeneJET Genomic DNA Purification kit. The quality and quantity of extracted phage and bacterial DNA were estimated using a NanoPhotometer and a Qubit fluorometer, respectively. The bacterial genome was sequenced at Plasmidsaurus (US). Five percent of the reads with the lowest quality were filtered out using Filtlong v0.2.1 (default) (https://github.com/rrwick/Filtlong). Miniasm v0.3 (*88*) was used to create a first draft of the assembly using a 250-Mb subset of reads. Low-quality reads were removed until a sequence depth of around 100× was achieved. Reads were assembled using Flye v2.9.1 (*89*) with parameters selected for high-quality ONT reads. Polishing of the assembly was conducted using Medaka v1.8.0 (https://github.com/nanoporetech/medaka) with the reads. Blastn v2.14.1 (*75*), with query coverage > 70% and pident > 70% was used to search for integrated temperate phages. Temperate phages were considered integrated in instances where the contig was at least 30% larger than the phage itself.

Fluorescence microscopy of defense systems

Exponentially growing ($OD_{600} \approx 0.3$) cultures of PAO1 strains containing pEmpty or the defense systems were infected with phage at an MOI ≥3, and the phage was adsorbed for 10 min at 37°C. Cells were centrifuged at 9,000*g* for 1 min, and the cell pellet was resuspended in 5 µl of 1 µM propidium iodide. The stained cells were spotted onto 1% agarose pads (*90*) and visualized using a Nikon Eclipse Ti2 inverted fluorescence microscope equipped with a 100× oil immersion objective (Nikon Apo TIRF; 1.49 numerical aperture). Time-lapse phase-contrast (CD Retiga R1) and fluorescence images (after excitation with a 561-nm laser 2000 609/54 bandpass filter, EM-CCD Andor iXON Ultra 897) were acquired every 5 min using Metamorph.

Statistical analysis

Unless stated otherwise, data are presented as the mean of biological triplicates ± SD. All correlation analyses were determined by linear (multiple) regression models using the lm function of R, and *P* values were adjusted with the Bonferroni post hoc test. The significance of differences between phylogenetic groups was determined using the Kruskal-Wallis test with Dunn's post hoc test, while the differences in infection dynamics were determined by two-way analysis of variance (ANOVA) followed by Sidak's multiple comparison test. For all statistical analyses, a significance level of 0.05 was used.

Supplementary Materials

This PDF file includes:

Figs. S1 to S9

Legends for tables S1 to S8

Other Supplementary Material for this manuscript includes the following:

Tables S1 to S8

REFERENCES AND NOTES

1. D. Piel, M. Bruto, Y. Labreuche, F. Blanquart, D. Goudenège, R. Barcia-Cruz, S. Chenivesse, S. le Panse, A. James, J. Dubert, B. Petton, E. Lieberman, K. M. Wegner, F. A. Hussain, K. M. Kauffman, M. F. Polz, D. Bikard, S. Gandon, E. P. C. Rocha, F. le Roux, Phage–host coevolution in natural populations. *Nat. Microbiol.* **7**, 1075–1086 (2022).
2. A. R. Burmeister, A. Fortier, C. Roush, A. J. Lessing, R. G. Bender, R. Barahman, R. Grant, B. K. Chan, P. E. Turner, Pleiotropy complicates a trade-off between phage resistance and antibiotic resistance. *Proc. Natl. Acad. Sci. U.S.A.* **117**, 11207–11216 (2020).
3. S. J. Labrie, J. E. Samson, S. Moineau, Bacteriophage resistance mechanisms. *Nat. Rev. Microbiol.* **8**, 317–327 (2010).
4. A. Bernheim, R. Sorek, The pan-immune system of bacteria: Antiviral defence as a community resource. *Nat. Rev. Microbiol.* **18**, 113–119 (2020).
5. H. G. Hampton, B. N. J. Watson, P. C. Fineran, The arms race between bacteria and their phage foes. *Nature* **577**, 327–336 (2020).
6. J. E. Egido, A. R. Costa, C. Aparicio-Maldonado, P.-J. Haas, S. J. J. Brouns, Mechanisms and clinical importance of bacteriophage resistance. *FEMS Microbiol. Rev.* **46**, fuab048 (2022).
7. R. Barrangou, C. Fremaux, Ĥ. Deveau, M. Richards, P. Boyaval, S. Moineau, D. A. Romero, P. Horvath, CRISPR Provides acquired resistance against viruses in prokaryotes. *Science* **315**, 1709–1712 (2007).
8. P. Mohanraju, K. S. Makarova, B. Zetsche, F. Zhang, E. V. Koonin, J. van der Oost, Diverse evolutionary roots and mechanistic variations of the CRISPR-Cas systems. *Science* **353**, aad5147 (2016).
9. T. A. Bickle, Restricting restriction. *Mol. Microbiol.* **51**, 3–5 (2004).
10. D. Dussoix, W. Arber, Host specificity of DNA produced by Escherichia coli. *J. Mol. Biol.* **5**, 37–49 (1962).
11. E. V. Koonin, K. S. Makarova, Y. I. Wolf, Evolutionary genomics of defense systems in archaea and bacteria. *Annu. Rev. Microbiol.* **71**, 233–261 (2017).
12. N. Tal, R. Sorek, SnapShot: Bacterial immunity. *Cell* **185**, 578–578.e1 (2022).
13. A. Millman, S. Melamed, A. Leavitt, S. Doron, A. Bernheim, J. Hör, J. Garb, N. Bechon, A. Brandis, A. Lopatina, G. Ofir, D. Hochhauser, A. Stokar-Avihail, N. Tal, S. Sharir, M. Voichek, Z. Erez, J. L. M. Ferrer, D. Dar, A. Kacen, G. Amitai, R. Sorek, An expanded arsenal of immune systems that protect bacteria from phages. *Cell Host Microbe* **30**, 1556–1569.e5 (2022).
14. C. Vassallo, C. Doering, M. L. Littlehale, G. Teodoro, M. T. Laub, Mapping the landscape of anti-phage defense mechanisms in the *E. coli* pangenome. bioRxiv 2022.05.12.491691 (2022). https://doi.org/10.1101/2022.05.12.491691.
15. F. A. Hussain, J. Dubert, J. Elsherbini, M. Murphy, D. VanInsberghe, P. Arevalo, K. Kauffman, B. K. Rodino-Janeiro, H. Gavin, A. Gomez, A. Lopatina, F. le Roux, M. F. Polz, Rapid evolutionary turnover of mobile genetic elements drives bacterial resistance to phages. *Science* **374**, 488–492 (2021).
16. F. Rousset, F. Depardieu, S. Miele, J. Dowding, A. L. Laval, E. Lieberman, D. Garry, E. P. C. Rocha, A. Bernheim, D. Bikard, Phages and their satellites encode hotspots of antiviral systems. *Cell Host Microbe* **30**, 740–753.e5 (2022).
17. F. Tesson, A. Hervé, E. Mordret, M. Touchon, C. d'Humières, J. Cury, A. Bernheim, Systematic and quantitative view of the antiviral arsenal of prokaryotes. *Nat. Commun.* **13**, 2561 (2022).
18. D. Subedi, A. K. Vijay, G. S. Kohli, S. A. Rice, M. Willcox, Comparative genomics of clinical strains of Pseudomonas aeruginosa strains isolated from different geographic sites. *Sci. Rep.* **8**, 15668 (2018).
19. V. Krylov, M. Bourkaltseva, E. Pleteneva, O. Shaburova, S. Krylov, A. Karaulov, S. Zhavoronok, O. Svitich, V. Zverev, Phage phiKZ-The First of Giants. *Viruses* **13**, 149 (2021).
20. H. Bin Jang, B. Bolduc, O. Zablocki, J. H. Kuhn, S. Roux, E. M. Adriaenssens, J. R. Brister, A. M. Kropinski, M. Krupovic, R. Lavigne, D. Turner, M. B. Sullivan, Taxonomic assignment of uncultivated prokaryotic virus genomes is enabled by gene-sharing networks. *Nat. Biotechnol.* **37**, 632–639 (2019).
21. M. Hunter, D. Fusco, Superinfection exclusion: A viral strategy with short-term benefits and long-term drawbacks. *PLoS Comput. Biol.* **18**, e1010125 (2022).
22. S. A. Jackson, N. Birkholz, L. M. Malone, P. C. Fineran, Imprecise spacer acquisition generates CRISPR-Cas immune diversity through primed adaptation. *Cell Host Microbe* **25**, 250–260.e4 (2019).
23. P. C. Fineran, M. J. H. Gerritzen, M. Suárez-Diez, T. Künne, J. Boekhorst, S. A. F. T. van Hijum, R. H. J. Staals, S. J. J. Brouns, Degenerate target sites mediate rapid primed CRISPR adaptation. *Proc. Natl. Acad. Sci. U.S.A.* **111**, E1629–E1638 (2014).
24. R. H. J. Staals, S. A. Jackson, A. Biswas, S. J. J. Brouns, C. M. Brown, P. C. Fineran, Interference-driven spacer acquisition is dominant over naive and primed adaptation in a native CRISPR–Cas system. *Nat. Commun.* **7**, 12853 (2016).
25. K. C. Cady, A. S. White, J. H. Hammond, M. D. Abendroth, R. S. G. Karthikeyan, P. Lalitha, M. E. Zegans, G. A. O'Toole, Prevalence, conservation and functional analysis of Yersinia and Escherichia CRISPR regions in clinical Pseudomonas aeruginosa isolates. *Microbiology* **157**, 430–437 (2011).
26. H. P. Schweizer, Escherichia-Pseudomonas shuttle vectors derived from pUC18/19. *Gene* **97**, 109–112 (1991).
27. L. A. Gao, M. E. Wilkinson, J. Strecker, K. S. Makarova, R. K. Macrae, E. V. Koonin, F. Zhang, Prokaryotic innate immunity through pattern recognition of conserved viral proteins. *Science* **377**, eabm4096 (2022).
28. E. Huiting, X. Cao, J. Ren, J. S. Athukoralage, Z. Luo, S. Silas, N. An, H. Carion, Y. Zhou, J. S. Fraser, Y. Feng, J. Bondy-Denomy, Bacteriophages inhibit and evade cGAS-like immune function in bacteria. *Cell* **186**, 864–876.e21 (2023).

29. T. Zhang, H. Tamman, K. Coppieters 't Wallant, T. Kurata, M. LeRoux, S. Srikant, T. Brodiazhenko, A. Cepauskas, A. Talavera, C. Martens, G. C. Atkinson, V. Hauryliuk, A. Garcia-Pino, M. T. Laub, Direct activation of a bacterial innate immune system by a viral capsid protein. *Nature* **612**, 132–140 (2022).
30. A. Stokar-Avihail, T. Fedorenko, J. Hör, J. Garb, A. Leavitt, A. Millman, G. Shulman, N. Wojtania, S. Melamed, G. Amitai, R. Sorek, Discovery of phage determinants that confer sensitivity to bacterial immune systems. *Cell* **186**, 1863–1876 (2023).
31. R. Cheng, F. Huang, X. Lu, Y. Yan, B. Yu, X. Wang, B. Zhu, Prokaryotic Gabija complex senses and executes nucleotide depletion and DNA cleavage for antiviral defense. *Cell Host Microbe* **31**, 1331–1344.e5 (2023).
32. C. K. Guegler, M. T. Laub, Shutoff of host transcription triggers a toxin-antitoxin system to cleave phage RNA and abort infection. *Mol. Cell* **81**, 2361–2373.e9 (2021).
33. A. Millman, A. Bernheim, A. Stokar-Avihail, T. Fedorenko, M. Voichek, A. Leavitt, Y. Oppenheimer-Shaanan, R. Sorek, Bacterial retrons function in anti-phage defense. *Cell* **183**, 1551–1561.e12 (2020).
34. Q. Ye, R. K. Lau, I. T. Mathews, E. A. Birkholz, J. D. Watrous, C. S. Azimi, J. Pogliano, M. Jain, K. D. Corbett, HORMA domain proteins and a Trip13-like ATPase regulate bacterial cGAS-like enzymes to mediate bacteriophage immunity. *Mol. Cell* **77**, 709–722.e7 (2020).
35. S. P. B. van Beljouw, J. Sanders, A. Rodríguez-Molina, S. J. J. Brouns, RNA-targeting CRISPR–Cas systems. *Nat. Rev. Microbiol.* **21**, 21–34 (2023).
36. V. Chaikeeratisak, K. Nguyen, K. Khanna, A. F. Brilot, M. L. Erb, J. K. C. Coker, A. Vavilina, G. L. Newton, R. Buschauer, K. Pogliano, E. Villa, D. A. Agard, J. Pogliano, Assembly of a nucleus-like structure during viral replication in bacteria. *Science* **355**, 194–197 (2017).
37. L. M. Malone, S. L. Warring, S. A. Jackson, C. Warnecke, P. P. Gardner, L. F. Gumy, P. C. Fineran, A jumbo phage that forms a nucleus-like structure evades CRISPR–Cas DNA targeting but is vulnerable to type III RNA-based immunity. *Nat. Microbiol.* **5**, 48–55 (2020).
38. S. D. Mendoza, E. S. Nieweglowska, S. Govindarajan, L. M. Leon, J. D. Berry, A. Tiwari, V. Chaikeeratisak, J. Pogliano, D. A. Agard, J. Bondy-Denomy, A bacteriophage nucleus-like compartment shields DNA from CRISPR nucleases. *Nature* **577**, 244–248 (2020).
39. S. A. McMahon, G. A. Roberts, K. A. Johnson, L. P. Cooper, H. Liu, J. H. White, L. G. Carter, B. Sanghvi, M. Oke, M. D. Walkinshaw, G. W. Blakely, J. H. Naismith, D. T. F. Dryden, Extensive DNA mimicry by the ArdA anti-restriction protein and its role in the spread of antibiotic resistance. *Nucleic Acids Res.* **37**, 4887–4897 (2009).
40. W. Liang, Y. Xie, W. Xiong, Y. Tang, G. Li, X. Jiang, Y. Lu, Anti-restriction protein, KlcAHS, promotes dissemination of carbapenem resistance. *Front. Cell. Infect. Microbiol.* **7**, (2017).
41. D. Serfiotis-Mitsa, A. P. Herbert, G. A. Roberts, D. C. Soares, J. H. White, G. W. Blakely, D. Uhrín, D. T. F. Dryden, The structure of the KlcA and ArdB proteins reveals a novel fold and antirestriction activity against Type I DNA restriction systems in vivo but not in vitro. *Nucleic Acids Res.* **38**, 1723–1737 (2010).
42. S. J. Hobbs, T. Wein, A. Lu, B. R. Morehouse, J. Schnabel, A. Leavitt, E. Yirmiya, R. Sorek, P. J. Kranzusch, Phage anti-CBASS and anti-Pycsar nucleases subvert bacterial immunity. *Nature* **605**, 522–526 (2022).
43. P. Ho, Y. Chen, S. Biswas, E. Canfield, D. E. Feldman, Bacteriophage anti-defense genes that neutralize TIR and STING immune responses. *Cell Rep.* **42**, 112305 (2022).
44. S. Shehreen, N. Birkholz, P. C. Fineran, C. M. Brown, Widespread repression of anti-CRISPR production by anti-CRISPR-associated proteins. *Nucleic Acids Res.* **50**, 8615–8625 (2022).
45. F. J. Whelan, M. Rusilowicz, J. O. McInerney, Coinfinder: Detecting significant associations and dissociations in pangenomes. *Microb. Genom.* **6**, e000338 (2020).
46. A. Lopatina, N. Tal, R. Sorek, Abortive infection: Bacterial suicide as an antiviral immune strategy. *Ann. Rev. Virol.* **7**, 371–384 (2020).
47. D. V. Banh, C. G. Roberts, A. M. Amador, S. F. Brady, L. A. Marraffini, Bacterial cGAS senses a viral RNA to initiate immunity. bioRxiv 2023.03.07.531596 (2023). https://doi.org/10.1101/2023.03.07.531596.
48. A. T. Whiteley, J. B. Eaglesham, C. C. de Oliveira Mann, B. R. Morehouse, B. Lowey, E. A. Nieminen, O. Danilchanka, D. S. King, A. S. Y. Lee, J. J. Mekalanos, P. J. Kranzusch, Bacterial cGAS-like enzymes synthesize diverse nucleotide signals. *Nature* **567**, 194–199 (2019).
49. M. C. Williams, A. E. Reker, S. R. Margolis, J. Liao, M. Wiedmann, E. R. Rojas, A. J. Meeske, Restriction endonuclease cleavage of phage DNA enables resuscitation from Cas13-induced bacterial dormancy. *Nat. Microbiol.* **8**, 400–409 (2023).
50. M. Jaskólska, D. W. Adams, M. Blokesch, Two defence systems eliminate plasmids from seventh pandemic Vibrio cholerae. *Nature* **604**, 323–329 (2022).
51. Y. Wu, Anne van den Hurk, C. Aparicio-Maldonado, S. K. Kushwaha, C. M. King, Y. Ou, T. C. Todeschini, M. R. J. Clokie, A. D. Millard, Y. E. Gençay, F. L. Nobrega, Defence systems provide synergistic anti-phage activity in *E. coli*. bioRxiv 2022.08.21.504612 (2022). https://doi.org/10.1101/2022.08.21.504612.
52. M.-È. Dupuis, M. Villion, A. H. Magadán, S. Moineau, CRISPR-Cas and restriction–modification systems are compatible and increase phage resistance. *Nat. Commun.* **4**, 2087 (2013).
53. N. Birkholz, S. A. Jackson, R. D. Fagerlund, P. C. Fineran, A mobile restriction–modification system provides phage defence and resolves an epigenetic conflict with an antagonistic endonuclease. *Nucleic Acids Res.* **50**, 3348–3361 (2022).
54. F. L. Nobrega, M. Vlot, P. A. de Jonge, L. L. Dreesens, H. J. E. Beaumont, R. Lavigne, B. E. Dutilh, S. J. J. Brouns, Targeting mechanisms of tailed bacteriophages. *Nat. Rev. Microbiol.* **16**, 760–773 (2018).
55. S. T. Abedon, Lysis from without. *Bacteriophage* **1**, 46–49 (2011).
56. R. R. Wick, L. M. Judd, C. L. Gorrie, K. E. Holt, Unicycler: Resolving bacterial genome assemblies from short and long sequencing reads. *PLoS Comput. Biol.* **13**, e1005595 (2017).
57. R. R. Wick, M. B. Schultz, J. Zobel, K. E. Holt, Bandage: Interactive visualization of de novo genome assemblies. *Bioinformatics* **31**, 3350–3352 (2015).
58. D. E. Wood, J. Lu, B. Langmead, Improved metagenomic analysis with Kraken 2. *Genome Biol.* **20**, 257 (2019).
59. S. Andrews. FastQC: A quality control tool for high throughput sequence data; www.bioinformatics.babraham.ac.uk/projects/fastqc/ (2010).
60. F. A. Simão, R. M. Waterhouse, P. Ioannidis, E. V. Kriventseva, E. M. Zdobnov, BUSCO: Assessing genome assembly and annotation completeness with single-copy orthologs. *Bioinformatics* **31**, 3210–3212 (2015).
61. H. Li, Minimap2: Pairwise alignment for nucleotide sequences. *Bioinformatics* **34**, 3094–3100 (2018).
62. P. Danecek, J. K. Bonfield, J. Liddle, J. Marshall, V. Ohan, M. O. Pollard, A. Whitwham, T. Keane, S. A. McCarthy, R. M. Davies, H. Li, Twelve years of SAMtools and BCFtools. *GigaScience* **10**, giab008 (2021).
63. H. Li, B. Handsaker, A. Wysoker, T. Fennell, J. Ruan, N. Homer, G. Marth, G. Abecasis, R. Durbin, 1000 Genome Project Data Processing Subgroup, The sequence alignment/map format and SAMtools. *Bioinformatics* **25**, 2078–2079 (2009).
64. D. Hyatt, G. L. Chen, P. F. LoCascio, M. L. Land, F. W. Larimer, L. J. Hauser, Prodigal: Prokaryotic gene recognition and translation initiation site identification. *BMC Bioinformatics* **11**, 119–119 (2010).
65. K. A. Jolley, M. C. J. Maiden, BIGSdb: Scalable analysis of bacterial genome variation at the population level. *BMC Bioinformatics* **11**, 595 (2010).
66. T. J. Treangen, B. D. Ondov, S. Koren, A. M. Phillippy, The Harvest suite for rapid core-genome alignment and visualization of thousands of intraspecific microbial genomes. *Genome Biol.* **15**, 524 (2014).
67. J. Guo, B. Bolduc, A. A. Zayed, A. Varsani, G. Dominguez-Huerta, T. O. Delmont, A. A. Pratama, M. C. Gazitúa, D. Vik, M. B. Sullivan, S. Roux, VirSorter2: A multi-classifier, expert-guided approach to detect diverse DNA and RNA viruses. *Microbiome* **9**, 37 (2021).
68. S. Nayfach, A. P. Camargo, F. Schulz, E. Eloe-Fadrosh, S. Roux, N. C. Kyrpides, CheckV assesses the quality and completeness of metagenome-assembled viral genomes. *Nat. Biotechnol.* **39**, 578–585 (2021).
69. R. K. Aziz, D. Bartels, A. A. Best, M. DeJongh, T. Disz, R. A. Edwards, K. Formsma, S. Gerdes, E. M. Glass, M. Kubal, F. Meyer, G. J. Olsen, R. Olson, A. L. Osterman, R. A. Overbeek, L. K. McNeil, D. Paarmann, T. Paczian, B. Parrello, G. D. Pusch, C. Reich, R. Stevens, O. Vassieva, V. Vonstein, A. Wilke, O. Zagnitko, The RAST server: Rapid annotations using subsystems technology. *BMC Genomics* **9**, 75 (2008).
70. J. R. Garneau, F. Depardieu, L.-C. Fortier, D. Bikard, M. Monot, PhageTerm: A tool for fast and accurate determination of phage termini and packaging mechanism using next-generation sequencing data. *Sci. Rep.* **7**, 8292 (2017).
71. P. Tynecki, A. Guziński, J. Kazimierczak, M. Jadczuk, J. Dastych, A. Onisko, PhageAI - bacteriophage life cycle recognition with machine learning and natural language processing. bioRxiv 2020.07.11.198606 (2020). https://doi.org/10.1101/2020.07.11.198606.
72. P. Aiewsakun, E. M. Adriaenssens, R. Lavigne, A. M. Kropinski, P. Simmonds, Evaluation of the genomic diversity of viruses infecting bacteria, archaea and eukaryotes using a common bioinformatic platform: Steps towards a unified taxonomy. *J. Gen. Virol.* **99**, 1331–1343 (2018).
73. P. Shannon, A. Markiel, O. Ozier, N. S. Baliga, J. T. Wang, D. Ramage, N. Amin, B. Schwikowski, T. Ideker, Cytoscape: A software environment for integrated models of biomolecular interaction networks. *Genome Res.* **13**, 2498–2504 (2003).
74. C. L. M. Gilchrist, Y.-H. Chooi, Clinker & clustermap. js: Automatic generation of gene cluster comparison figures. *Bioinformatics* **37**, 2473–2475 (2021).
75. S. F. Altschul, W. Gish, W. Miller, E. W. Myers, D. J. Lipman, Basic local alignment search tool. *J. Mol. Biol.* **215**, 403–410 (1990).
76. L. J. Payne, T. C. Todeschini, Y. Wu, B. J. Perry, C. W. Ronson, P. C. Fineran, F. L. Nobrega, S. A. Jackson, Identification and classification of antiviral defence systems in bacteria and archaea with PADLOC reveals new system types. *Nucleic Acids Res.* **49**, 10868–10878 (2021).
77. L. Gao, H. Altae-Tran, F. Böhning, K. S. Makarova, M. Segel, J. L. Schmid-Burgk, J. Koob, Y. I. Wolf, E. V. Koonin, F. Zhang, Diverse enzymatic activities mediate antiviral immunity in prokaryotes. *Science* **369**, 1077–1084 (2020).

78. F. Rousset, E. Yirmiya, S. Nesher, A. Brandis, T. Mehlman, M. Itkin, S. Malitsky, A. Millman, S. Melamed, R. Sorek, A conserved family of immune effectors cleaves cellular ATP upon viral infection. *Cell* **186**, 3619–3631.e13 (2023).
79. A. Biswas, R. H. J. Staals, S. E. Morales, P. C. Fineran, C. M. Brown, CRISPRDetect: A flexible algorithm to define CRISPR arrays. *BMC Genomics* **17**, 356–356 (2016).
80. H. Yi, L. Huang, B. Yang, J. Gomez, H. Zhang, Y. Yin, AcrFinder: Genome mining anti-CRISPR operons in prokaryotes and their viruses. *Nucleic Acids Res.* **48**, W358–W365 (2020).
81. S. F. Altschul, T. L. Madden, A. A. Schäffer, J. Zhang, Z. Zhang, W. Miller, D. J. Lipman, Gapped BLAST and PSI-BLAST: A new generation of protein database search programs. *Nucleic Acids Res.* **25**, 3389–3402 (1997).
82. R. D. Finn, J. Clements, S. R. Eddy, HMMER web server: Interactive sequence similarity searching. *Nucleic Acids Res.* **39**, W29–W37 (2011).
83. J. Söding, A. Biegert, A. N. Lupas, The HHpred interactive server for protein homology detection and structure prediction. *Nucleic Acids Res.* **33**, W244–W248 (2005).
84. K.-H. Choi, A. Kumar, H. P. Schweizer, A 10-min method for preparation of highly electrocompetent Pseudomonas aeruginosa cells: Application for DNA fragment transfer between chromosomes and plasmid transformation. *J. Microbiol. Methods* **64**, 391–397 (2006).
85. E.-M. Lammens, M. Boon, D. Grimon, Y. Briers, R. Lavigne, SEVAtile: A standardised DNA assembly method optimised for Pseudomonas. *J. Microbial. Biotechnol.* **15**, 370–386 (2022).
86. A. Mazzocco, T. E. Waddell, E. Lingohr, R. P. Johnson, in *Bacteriophages: Methods and Protocols*, vol. 1, *Isolation, Characterization, and Interactions*, M. R. J. Clokie, A. M. Kropinski, Eds. (Humana Press, 2009), pp. 81–85.
87. A. M. Kropinski, A. Mazzocco, T. E. Waddell, E. Lingohr, R. P. Johnson, in *Bacteriophages: Methods and Protocols*, vol. 1, *Isolation, Characterization, and Interactions*, M. R. J. Clokie, A. M. Kropinski, Eds. (Humana Press, 2009), pp. 69–76.
88. H. Li, Minimap and miniasm: Fast mapping and de novo assembly for noisy long sequences. *Bioinformatics* **32**, 2103–2110 (2016).
89. M. Kolmogorov, J. Yuan, Y. Lin, P. A. Pevzner, Assembly of long, error-prone reads using repeat graphs. *Nat. Biotechnol.* **37**, 540–546 (2019).
90. J. N. A. Vink, S. J. J. Brouns, J. Hohlbein, Extracting transition rates in particle tracking using analytical diffusion distribution analysis. *Biophys. J.* **119**, 1970–1983 (2020).

Acknowledgments: We thank L. Gao and F. Zhang (Massachusetts Institute of Technology) for providing the HMMs for the detection of defense systems, and W. Song and M. Xiao (BGI-Shenzhen) for sequencing part of the clinical isolates and phages used in this study. We would like to thank W. de Leeuw and H. Rauwerda (University of Amsterdam, Swammerdam Institute for Life Sciences, MAD/RB&AB) for the use of the Crunchomics computer cluster, and R. Lavigne from KU Leuven for providing plasmid pSTDesR. We also thank members of the Brounslab for the many discussions and ideas that improved our work. **Funding:** This work was supported by the European Research Council (ERC) CoG grant no. 101003229 and the Netherlands Organisation for Scientific Research VICI grant VI.C.192.027, to S.J.J.B. **Author contributions:** Conceptualization: S.J.J.B. Methodology: S.J.J.B., F.L.N., A.R.C., and D.F.v.d.B. Software: D.F.v.d.B. and A.M. Formal analysis: A.R.C., D.F.v.d.B., J.Q.E., A.M., B.A.v.d.S., and H.v.d.B. Investigation: A.R.C., D.F.v.d.B., J.Q.E., A.M., H.v.d.B., B.E.B., and A.C.H. Visualization: A.R.C., D.F.v.d.B., J.Q.E., H.v.d.B., and A.M. Data Curation: A.R.C., D.F.v.d.B., and J.Q.E. Writing—original draft: A.R.C., D.F.v.d.B., J.Q.E. Writing—review & editing: S.J.J.B. Resources: P.-J.H., A.C.F., F.L.N., and S.J.J.B. Funding aquisition: S.J.J.B. **Competing interests:** The authors declare that they have no competing interests. **Data and materials availability:** All data needed to evaluate the conclusions in the paper are present in the paper, the Supplementary Materials, or at Zenodo (www.doi.org/10.5281/zenodo.8405451). All original code has been deposited at Zenodo and GitHub (https://github.com/BrounsLab-TUDelft/Pseudomonas_Defence_Systems). Raw data and assembled bacterial and phage genomes are available from GenBank, Bioproject PRJNA817167 (individual accession numbers are listed in tables S2 and S3). Plasmid pSTDesR can be provided pending scientific review and a completed material transfer agreement. Requests for pSTDesR should be submitted to R. Lavigne, KU Leuven.

Submitted 2 June 2023
Accepted 22 January 2024
Published 23 February 2024
10.1126/sciadv.adj0341